Structural Regulation of a Peptide-Conjugated Graft Copolymer: A Simple Model for Amyloid Formation

Tomoyuki Koga,[a] Kazuhiro Taguchi,[a] Yoshiaki Kobuke,[b] Takatoshi Kinoshita,[c] and Masahiro Higuchi*[a]

Abstract: The self-assembly of peptides and proteins into β-sheet-rich high-order structures has attracted much attention as a result of the characteristic nanostructure of these assemblies and because of their association with neurodegenerative diseases. Here we report the structural and conformational properties of a peptide-conjugated graft copolymer, poly(γ-methyl-L-glutamate) grafted polyallylamine (**1**) in a water-2,2,2-trifluoroethanol solution as a simple model for amyloid formation. Atomic force microscopy revealed that the globular peptide **1** self-assembles into nonbranching fibrils that are about 4 nm in height under certain conditions. These fibrils are rich in β-sheets and, similar to authentic amyloid fibrils, bind the amyloidophilic dye Congo red. The secondary and quaternary structures of the peptide **1** can be controlled by manipulating the pH, solution composition, and salt concentration; this indicates that the three-dimensional packing arrangement of peptide chains is the key factor for such fibril formation. Furthermore, the addition of carboxylic acid-terminated poly(ethylene glycol), which interacts with both of amino groups of **1** and hydrophobic PMLG chains, was found to obviously inhibit the α-to-β structural transition for non-assembled peptide **1** and to partially cause a β-to-α structural transition against the **1**-assembly in the β-sheet form. These findings demonstrate that the amyloid fibril formation is not restricted to specific protein sequences but rather is a generic property of peptides. The ability to control the assembled structure of the peptide should provide useful information not only for understanding the amyloid fibril formation, but also for developing novel peptide-based material with well-defined nanostructures.

Keywords: amyloid · conformation analysis · graft-copolymer · peptide · self-assembly

Introduction

α-Helices and β-sheets are the major secondary structural motifs organizing the three-dimensional geometry of proteins. It is generally considered that the sequence of amino acids is important in shaping the properties of the protein secondary structure, and that the secondary structures are stable once they have formed.[1–3] The protein quaternary structure formed by the organization of such secondary structural elements plays a key role in defining their functions and different nature. In this regard, much recent effort has been directed toward elucidating the interactions between peptides involved in protein folding, and toward developing protein-based material. In particular, the self-assembly of peptides and proteins into β-sheet-rich fibrillar structures (called amyloid fibrils) is currently the focus of biochemical and biophysical research because of their association with neurodegenerative diseases such as the Alzheimer's disease and Creutzfeldt–Jacob disease.[4–8] Many investigators believe that protein conformation changes, rather than the specific primary structure of the proteins, are central to the disease process. In fact, neurotoxic effects of disease-related amyloid peptides have been reported to depend on their conformation and physical state in some cases.[9–11] However, despite extensive studies of amyloid fibrils that have resulted in the elucidation of many aspects of their underlying nature, important issues concerning their structure and mechanism of formation remain to be resolved. Thus, it is important to construct peptide β-sheet assemblies and elucidate their molecular-level structure in order to understand the pathogenesis of and therapeutics for the diseases with which they are associated.

[a] Dr. M. Higuchi, Dr. T. Koga, Dr. K. Taguchi
Nanoarchitectonics Research Center
National Institute of Advanced Industrial Science and Technology and CREST (Japan Science and Technology)
Tsukuba Central 5, 1-1-1 Higashi, Tsukuba
Ibaraki 305-8565 (Japan)
Fax: (+81) 298 61 4682
E-mail: m.higuchi@aist.go.jp

[b] Prof. Y. Kobuke
Graduate School of Materials Science
Nara Institute of Science and Technology
and CREST (Japan Science and Technology) (Japan)

[c] Prof. T. Kinoshita
Department of Materials Science and Engineering
Nagoya Institute of Technology
and CREST (Japan Science and Technology) (Japan)

0947-6539/03/0905-1146 $ 20.00+.50/0

In previous studies, a total of at least 16 different proteins and peptides were identified in amyloid aggregates,[5, 12] and these aggregates were found to have a common core structure despite the fact that the proteins involved have no sequential or structural similarities. For example, all amyloids are long, straight, and unbranched; their diameter ranges between 40–120 Å, and they exhibit a cross β-sheet structure in which continuous β-sheets lie parallel to the long axis of a fiber and their constituent β-strands run perpendicular to this axis.[13] Recently, Dobson et al. found that non-pathogenic proteins, including those of the SH3 domain,[14] acylphosphatase,[15] and apo-myoglobin,[16] also form amyloid fibrils in vitro under certain conditions, and suggested that the formation of amyloid fibrils is a genetic property of the peptides and proteins.

In synthetic systems, various peptides were also reported to form amyloid-like β-sheet assemblies in vitro that structurally resemble in situ fibrils.[17–21] Thus, the ability to form amyloid fibrils from a wide range of synthetic peptides provides access to a large number of model systems which can be used to study the fibril formation in greater detail. In addition, these synthetic peptide assemblies with a well-defined nanostructure are also interesting from a supramolecular point of view. These self-assembled polymeric architectures are expected to possess potential as novel biomaterials with a wide range of applications, such as use in nanodevices.[22–24]

In this paper, we prepared a simple artificial protein with an α-helical homo-polypeptide, poly(γ-methyl-L-glutamate)-conjugated polyallylamine (**1**), as a simple model for amyloid formation. A detailed analysis of the conformation and morphology in solution was performed in consideration of both environmental conditions and intermolecular interaction with poly(ethylene glycol) derivatives. These studies should provide simple and/or essential insight into the mechanism of peptide aggregation including amyloid formation and should be useful for the design of novel peptide-based nanomaterials.

Results

Design and synthesis of artificial protein model: To obtain simple and/or essential information about the protein misfoldings and aggregation involved in amyloid formation, we prepared an artificial peptide with a simple primary structure as a high-order structural model of proteins. Protein tertiary structures can be looked upon as assemblies of secondary structural elements (for example, α-helices, β-strands, and reversed turns) connected by flexible loops. This model has been the basis for the design of artificial proteins. The design process is simple; secondary structure modules are created and then connected together with appropriate loops. A recent approach for artificial protein design involves the use of template molecules such as metal ligands, rigid plane molecules, dendrimers.[27–33] Many artificial proteins have been prepared in aqueous solutions by attaching peptide blocks to templates that direct the component helices into protein-like packing arrangements. We chose a poly(γ-methyl-L-glutamate) (PMLG) as a secondary structure module because of its easy synthesis and well-defined conformational characteristics in solution, and chose a polyallylamine (PAA) as both a flexible template for assembly and an initiator for graft-polymerization.[34] In addition, we anticipated that it might be possible to control the distribution of the quaternary structures by manipulating solution composition, pH, ionic strength, and the like, owing to perturbations of peptide chains dependent on the pK_a of the PAA amino groups.

The synthesis of the artificial protein, PMLG-grafted PAA (**1**), is outlined in Scheme 1. First, amino groups of PAA were partially protected with Boc groups by treating the PAA with

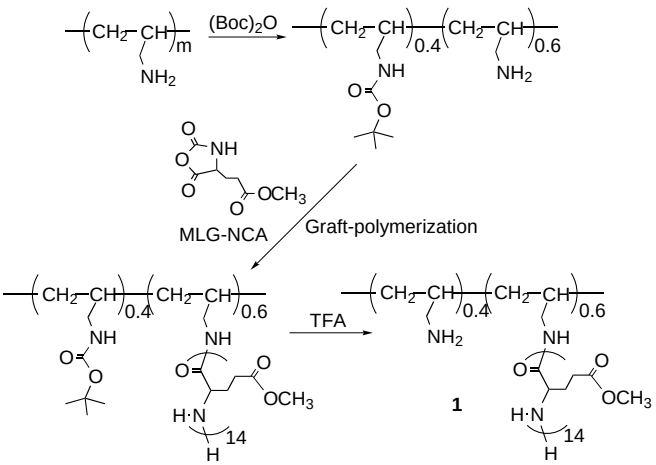

Scheme 1. Synthetic route of an artificial amyloidgenic peptide, poly(γ-methyl-L-glutamate) grafted-polyallylamine (**1**). Boc: *tert*-butoxy carbonyl, TFA: tri-fluoroacetic acid.

di-*tert*-butyl dicarbonate in a water/dioxane solution. The degree of the reaction of amino groups was successfully controlled by adjusting the feed ratio of di-*tert*-butyl dicarbonate to amino groups. As a result, the PAA copolymer was prepared in which the amino groups (40%) were protected with Boc groups. Next, the graft-polymerization of γ-methyl-L-glutamate-*N*-carboxy anhydride was carried out using free amino groups of this PAA copolymer in chloroform. A relatively short chain length of the peptide segment (degree of polymerization $n = 10–15$) was employed because the number of amino acid unit is appropriate for both characterization of the resultant graft-polymer and elucidation of the effect of self-assembly. The graft-polymerization was found to proceed for all amino groups located on the PAA copolymer. The number-average degree of polymerization of the PMLG chain was determined to be 14 from ^{1}H NMR spectroscopy and elemental analysis. Finally, the desired peptide **1** was obtained by removal of the Boc groups in a trifluoroacetic acid solution.

Conformational properties of peptide-conjugated copolymer in solutions: The conformational properties of the peptide **1** in different solutions were first investigated by means of far-ultraviolet circular dichroism (far-UV CD) and Fourier-transform infrared (FTIR) spectroscopies. Figure 1A) shows the time dependence of far-UV CD spectra for peptide **1** at pH 4.0 after dilution in water from the TFE stock solution

  0947-6539/03/0905-1147 $ 20.00+.50/0

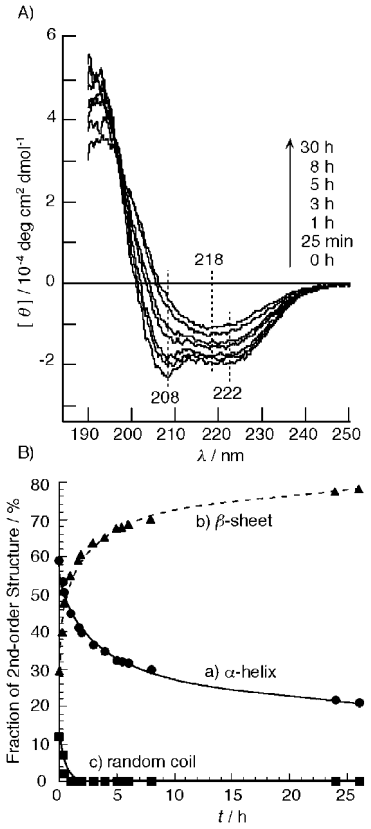

Figure 1. A) Far-UV CD spectral change of **1** in water/TFE (8:2 *v/v*) at pH 4.0. The peptide **1** was incubated at room temperature within the period indicated (0–30 h). [MLG] = 1.1×10^{-4} unit M. B) Time dependence of fraction of second-order structure a) α-helix structure, b) β-sheet structure, c) random coil structure) of **1** estimated from the CD-curve fitting method.

(final peptide concentration 1.1×10^{-4} glutamate unit M, TFE content 20%, no salt).

When the sample solution was freshly prepared, the spectrum gave a typical pattern of right-handed α-helical polypeptide with two negative maxima, at 222 and 208 nm. A quantitative curve-fitting analysis of the spectrum gave the following percentage of secondary structures: 59% of α-helix, 29% of β-sheet, 12% of random coil. This helicity is reasonable taking into account the relatively short segment length ($n = 14$). The far-UV CD measurements revealed a gradual change in a spectrum typical for a β-sheet structure, with a single negative maximum at 218 nm and a positive maximum at 197 nm after 30 h. These spectral changes within the incubation time are found to proceed through an isodichroic point at around 198 nm. Figure 1B) displays the percentage of secondary structures of PMLG segments evaluated using the CD-curve fitting method as a function of the incubation time under this condition. With time, the structural transition from α-helix to β-sheet proceeded without a lag phase, and reached values of about 20% of α-helix and about 78% of β-sheet after 26 h. This α-to-β transition was also observed at lower pH region (< 8, 20% TFE, no salt). On the other hand, at higher pH region (> 8), the far-UV CD spectra showed the typical α-helix pattern (negative maxima at 222 and 208 nm) even after 30 h, although the molar ellipticity was reduced to half its initial value (data not shown). This reduction in ellipticity was probably caused by the large aggregation of peptide **1**[35] suggested by fluorescence and atomic force microscopy studies (details described later). Far-UV CD studies in solution agree with FTIR experiments on films, and refer to the description of the FTIR experiments later on in the paper. The acid dissociation constant (pK_a) value of allylamine moiety was estimated to be 8.0 from potentiometric analysis.[34] On the other hand, the peptide chains (PMLG) involved have no pH-responsible residues except the N-terminus amino groups. Therefore, the observed pH-dependent difference in conformational properties of peptide **1** would be attributable to the three-dimensional packing arrangement of PMLG chains influenced by the protonation of amino groups.

In order to evaluate the effect of environmental conditions (solution composition, pH, and salt concentration) on conformational properties, the kinetics of the α-to-β structural transition for peptide **1** were subsequently investigated. We then focused on the time course of helicity decrease as estimated from CD analysis (for example, Figure 1B (a)), and the results were analyzed using a first-order kinetic model according to Equation (1):

$$\log(A/\Delta h(t)) = kt/2.303 \quad (1)$$

where $\Delta h(t)$ is the degree of helicity change of **1** as a function of time, A is tentatively determined as $\Delta h(t)$ at $t = \infty$ ($\Delta h(\infty)$) from hyperbolic curve of helicity, and k is the apparent initial rate of α-to-β structural transition. Figure 2 shows the plot of the value $log\ (A/\Delta h(t))$ versus incubation

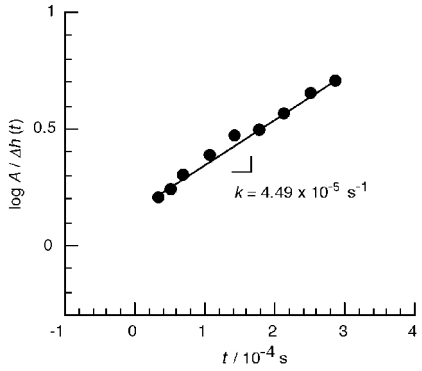

Figure 2. The plot of the value $\log A/\Delta h(t)$ versus incubation time of the peptide **1** in water/TFE (8:2 *v/v*, pH 4.0, no salt). $\Delta h(t)$ is the amount of helicity change in **1** as a function of time. A is tentatively determined as $\Delta h(t)$ at $t = 0$ ($\Delta h(\infty)$) from the hyperbolic curve shown in Figure 1B a). Linear least-square fitting was performed for the straight line ($r = 0.993$).

time of the peptide **1** in water/TFE (8:2 *v/v*, pH 4.0, no salt). In this figure, a linear relation ($r = 0.993$) is observed, indicating the first-order structural transition of the peptide **1**. The slope of this plot ($k = 4.49 \times 10^{-5}\ s^{-1}$) indicates the apparent initial rate of α-to-β conversion under this condition. The same analyses were conducted under various conditions, and the results are summarized in Table 1. The addition of TFE, which would weaken the hydrophobic interaction between PMLG chains, obviously decreased the transition rate with increasing TFE concentration. When more than 25% TFE was added,

0947-6539/03/0905-1148 $ 20.00+.50/0 *Chem. Eur. J.* **2003**, *9*, No. 5

Table 1. Effects of environmental conditions on the secondary structure and initial rate of α-to-β structural transition for the peptide **1**.

Conditions[a]		Initial rate of α-to-β structural transition [s^{-1}]	Secondary structure[b]
TFE content [%][c]	18	1.16×10^{-4}	β-sheet
	20	4.49×10^{-5}	β-sheet
	23	9.63×10^{-6}	β-sheet
	25	3.06×10^{-6}	β-sheet
	30	–	α-helix
	40	–	α-helix
	50	–	α-helix
	100	–	α-helix
pH[d]	4.00	4.49×10^{-5}	β-sheet
	4.67	7.35×10^{-5}	β-sheet
	5.38	8.21×10^{-5}	β-sheet
	7.30	1.02×10^{-4}	β-sheet
	8.70	–	α-helix
	9.20	–	α-helix
	9.56	–	α-helix
	9.74	–	α-helix
salt[e] (NaCl) [mM]	0	4.49×10^{-5}	β-sheet
	2	4.32×10^{-5}	β-sheet
	5	5.25×10^{-5}	β-sheet
	10	5.72×10^{-5}	β-sheet
	30	2.09×10^{-5}	β-sheet
	50	–	α-helix
	200	–	α-helix

[a] All experiments were performed at room temperature and the constant peptide concentration 1.1×10^{-4} glutamate unit M. [b] Secondary structure of the peptide segment was evaluated from far-UV CD spectroscopy after incubation of the peptide **1** for 48 h in aqueous solution. [c] Effect of solution composition on conformational properties were examined by varying the TFE content at pH 4.0, [NaCl] = 0 mM. [d] Experiments were conducted under the following conditions: TFE content = 20% (in vol.), [NaCl] = 0 mM. pH of the solution was adjusted with 0.1M HCl or 0.1M aqueous NaOH. [e] pH 4.0, TFE content = 20% (in vol.).

the α-to-β transition did not occur (no change was observed for the far-UV CD spectra after incubation for 48 h). The helicity obtained just after preparation of sample solutions was increased to 68% in 25% TFE in comparison with 59% in 20% TFE. It has been reported that for a medium-sized polypeptide, a small amount of TFE in water acts by diminishing the stabilization of water-exposed amide functions, shifting equilibrium away from the highly solvated coil state toward compact states that contain internally hydrogen-bonded or solvent-sequestered amides.[36–38] Therefore, it can be concluded that TFE increased the stability of the α-helix structure of PMLGs, and prevented the peptide aggregation that would have caused conformational transition into the β-sheet as a result of the weakness of the hydrophobic interaction between PMLGs.

The conformational properties of **1** were influenced by pH, where in turn could induced the perturbation of a high-order structure (tertiary and/or quaternary structures) in response to the charged condition of amino groups of **1**, as already described. The α-to-β transition rate increased with increasing pH up to 7.3. The highest transition rate was found to occur at neutral pH, where the peptide **1** possesses net positive charges, indicating the existence of an optimum packing arrangement for the α-to-β transition. Above pH 8.0, which is the pK_a value of allylamine moiety, the conformational transition did not take place. In this case, however, an aggregate formation of **1** without the α-to-β conformational transition was observed (reduction of the molar ellipticity to half its initial value after incubation), in contrast to the case of high TFE contents.

The addition of NaCl also influenced the conformation of **1** in a concentration-dependent manner. At lower NaCl concentration regions (< 10 mM), the α-to-β structural transition rate did not change significantly. On the other hand, at higher NaCl concentration regions (> 50 mM) the transition was retarded in a manner similar to that seen in the higher pH region. These results suggest that the distribution of high-order structures of peptide **1** could be easily controlled by manipulating environmental conditions such as solution composition, pH, and ionic strength.

Characterizing the aggregation behavior of peptide-conjugated copolymer by fluorescence spectroscopy and atomic force microscopy: To gain insight into the process of aggregate formation by peptide **1**, we followed its assembly as a function of time by fluorescence spectroscopy and atomic force microscopy (AFM). For the fluorescence spectroscopy study, we synthesized two fluorescent derivatives of **1**, containing a small nitrobenzofurazan (NBD) or rhodamine B (RhB) group at the amino groups of PAA segments (ca. 5% in both cases), to use as donors and acceptors, respectively. First, fluorescent resonance energy transfer (FRET) between NBD and RhB was used to monitor the association of peptide derivatives of **1** following dilution of TFE into aqueous solution. For these experiments, **1**-NBD and **1**-RhB TFE stock solutions were mixed 1:1 (donor/acceptor), then subsequently diluted five-fold in water or TFE at various conditions. Final peptide concentration was 1.1×10^{-4} glutamate unit M. Figure 3A shows fluorescence spectral changes of the mixture of **1**-NBD and **1**-RhB (1:1) in water/TFE (8:2 *v*/*v*) at pH 4.0 and in TFE. In a TFE solution, fluorescence emission of NBD was only observed at 533 nm, and this spectrum did not change even after incubation for 48 h (Figure 3A c) and d)), indicating that the peptide exists in TFE as a monomer. In contrast, in water/TFE (8:2 *v*/*v*) at pH 4.0, efficient FRET was observed, as evidenced by a quenching of the donor emission at 533 nm and an increase in the acceptor fluorescence at 567 nm (Figure 3A a)), as compared with the pure **1**-NBD observed under the same condition. The efficiency of FRET increased significantly upon subsequent incubation for 48 h (Figure 3A b)). This result indicates that association occurred between peptide derivatives **1** in the mixture containing both donor and acceptor. Figure 3B plots the time dependence of the I_{Rhb}/I_{NBD}, the ratio of emission intensity of **1**-RhB to that of **1**-NBD at various conditions. Whereas no change of the ratio of I_{Rhb}/I_{NBD} (0.50) was observed in TFE (Figure 3B c)), the ratio increased continuously with time and reached a constant value (from 0.81 to 1.05) at about 5 h in aqueous solution at pH 4.0 (Figure 3B a)). This time course of I_{Rhb}/I_{NBD} corresponded well to that of the α-to-β structural transition, indicating a strong relation between aggregate formation and conformational transition of peptide **1**. At pH 9.2, at which the

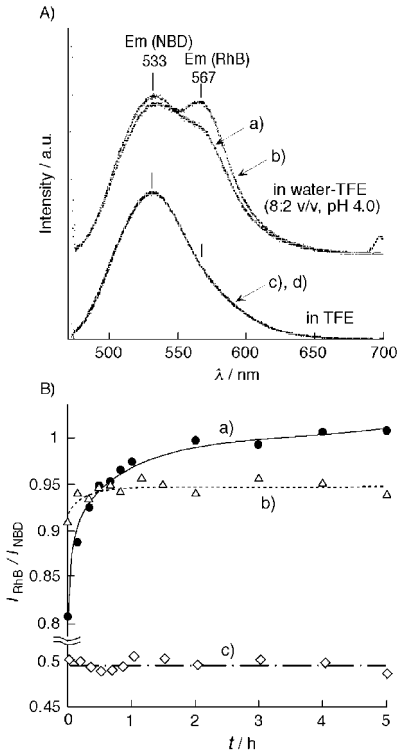

Figure 3. A) Fluorescence spectral changes of the mixture of **1**-NBD and **1**-RhB (1:1 in peptide concentration) in water/TFE (8:2 *v*/*v*) at pH 4.0 (a and b) and in TFE (c and d). The spectra were measured just after preparation of sample solutions (a and c) and after incubation for 48 h at room temperature (b and d). The total peptide concentration was 1.1×10^{-4} glutamate unit M. $\lambda_{ex} = 465$ nm. B) Time dependence of I_{RhB}/I_{NBD}, the ratio of emission intensity of **1**-RhB to that of **1**-NBD, in water/TFE (8:2 *v*/*v*) at pH 4.0 (a), 9.2 (b) and in TFE (c).

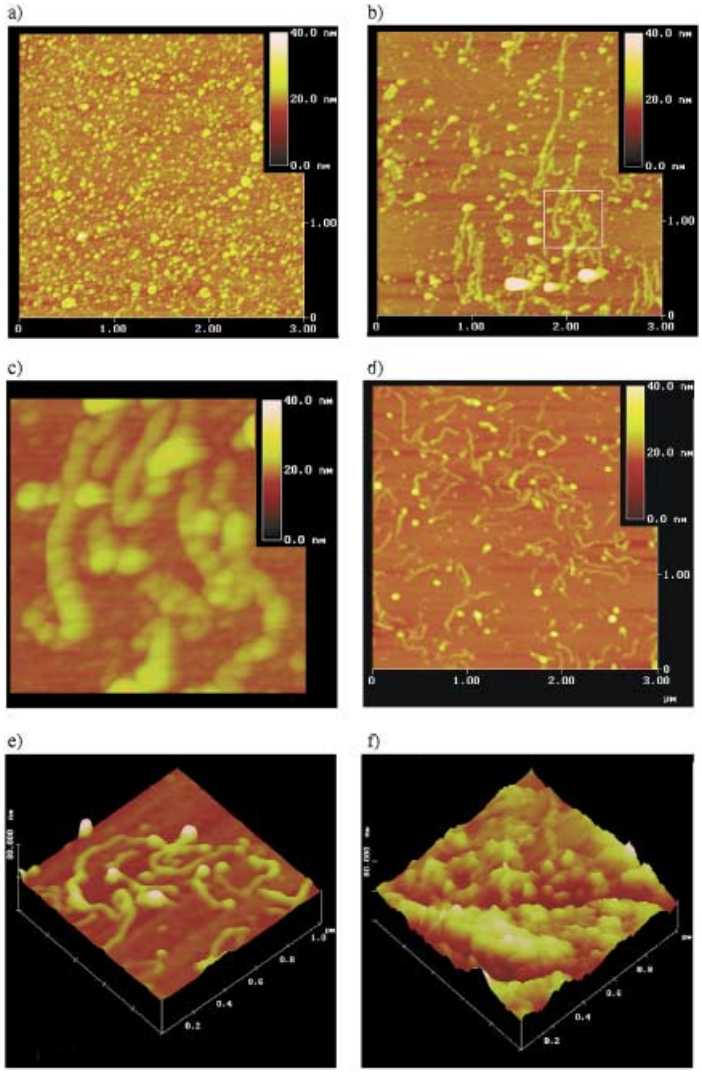

Figure 4. Time dependence of tapping mode AFM images (3 μm × 3 μm) for peptide **1**. The peptide **1** was incubated for 0 h (a), 5 h (b, c), and 48 h (d) in water/TFE (8:2 *v*/*v*) (pH 4.0) at room temperature. The image c corresponds to the area marked with square in image b. The images e and f show the three-dimensional height images (1 μm × 1 μm) of **1** after incubation for 48 h at pH 4.0 and 9.2, respectively; *z* scale: 0–40 nm. $[MLG] = 1.1 \times 10^{-4}$ unit M.

α-to-β structural transition of **1** did not occur, FRET was also observed just after preparation of sample solution (Figure 3B b)). The initial value of I_{Rhb}/I_{NBD} at pH 9.2 was higher (0.92) than that in TFE (0.50) or in aqueous solution at pH 4.0 (0.81); the intensity ratio did not increase significantly with incubation time, despite a rapid and slight increase of the value within 20 min. These results suggest that a large aggregation of **1** was formed rapidly at pH 9.2, but the additional aggregations which were observed at pH 4.0 did not proceed.

Subsequently, the morphological change with an aggregate formation of **1** (suggested by the FRET study) was investigated directly using the AFM technique. In the field of structural biology, AFM is a useful technique to evaluate the three-dimensional structural features of proteins and their assemblies. It is, however, well known that the convolution of the scanning tip leads to an overestimation of the sample's width.[39] All sample dimensions were therefore estimated from the height of the sample in the cross section. Figure 4 shows the time dependence of AFM images ($3 \times 3\ \mu m^2$) for peptide **1** at pH 4.0 (Figure 4a–e) and 9.2 (Figure 4f). An AFM image obtained just after the sample solution was prepared (0 h), in which the PMLG graft chain took mainly the α-helical form, revealed the presence of only nonfibrillar, globular aggregates (Figure 4a). The average height of the globular species was determined to be 6.0 ± 1.0 nm, and the width was typically 40–70 nm (AFM level). On the other hand, after incubation for 5 h, **1**-protofibrils (average height 4.5 ± 1.0 nm) were newly observed together with the globular species (Figure 4b). Harper et al. recently reported that the amyloid β-peptide (Aβ) protofibril elongation involved both the incorporation of monomers and the association of immature protofibrils.[40] As shown in Figure 4c, in our case, the protofibrils were characterized by a clearly periodic substructure, based on the finding that they were spaced at 30 ± 10 nm intervals along the protofibrils axis and that the difference between the maximum and minimum heights along the axis was 0.7 ± 0.4 nm. Therefore, this observation (i.e., the similarity of shape and size between the substructures of protofibrils and globular species) supports the idea that protofibrils of **1** are, like the authentic amyloid fibrils (Aβ), formed through the association of globular species. For 48 h after incubation, the major portion of **1** was found to form

0947-6539/03/0905-1150 $ 20.00+.50/0 *Chem. Eur. J.* **2003**, *9*, No. 5

amyloid-like fibril structures with an average height of 4.0 ± 1.0 nm and a length of 0.3–1.0 μm (Figure 4d, e). These dimensions were in fair agreement with those of typical amyloids.[13] In contrast, an amorphous large aggregate was observed, rather than such amyloid-like fibril structures for peptide **1** at pH 9.2; that is, at a pH at which rapid aggregation of **1** without α-to-β structural transition was observed (Figure 4f). These results show that the fibril formation of peptides **1** was closely related to their conformation and their association behavior. Furthermore, it should be noted that the purely synthetic graft-polymer **1** which have no specific protein sequences formed an amyloid-like fibril structure with structural transition under appropriate conditions, as did the other proteins associated with neurodegenerative diseases.

Characterization of fibril structure: Using resolved FTIR spectra, we determined the conformation and orientation of the secondary structural element (β-sheet) included in the fibril. Figure 5 shows the transmission (TM) and reflection

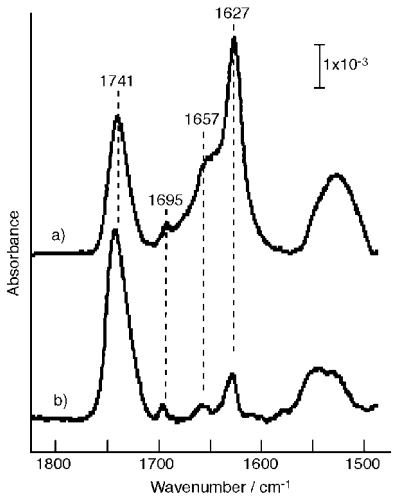

Figure 5. a) Transmission- and b) reflection absorption-FTIR spectra of the peptide **1**-fibril on CaF_2 plate and Au plate, respectively. The fibrillar **1** assembly was obtained after 48 h incubation in water/TFE (8:2 *v*/*v*) at pH 4.0.

absorption (RA) FTIR spectra of the fibril films of **1** on CaF_2 plate and gold plate, respectively. These films were obtained by adsorbing the peptide **1** after incubation for 48 h in water/TFE (8:2 *v*/*v*) at pH 4.0. To obtain quantitative information about secondary structure, we focused mainly on two bands assigned to the amide I and amide II of peptide main chain in TM-FTIR spectrum.[41] In the case of pH 4.0, characteristic absorptions of amide I and II bands with the antiparallel β-sheet structure were observed at 1695, 1627, and 1518 cm^{-1} (Figure 5a), whereas peptide **1** took mainly the α-helix structure (peak maxima at 1656 cm^{-1}, shoulder at 1627 cm^{-1} for amide I and 1558 cm^{-1} for amide II) at pH 9.2 (data not shown). The β-sheet contents were evaluated to be 77 and 34% at pH 4.0 and 9.2, respectively, from the ratio of integrated peak intensities assigned to a β-sheet conformation to that of α-helical and random conformation, which were obtained by peak deconvolution of the amide I and II bands, respectively.[41] These values were consistent with the results of far-UV CD measurements of peptide **1** in solutions.

In addition, it was found from Figure 5 that the intensity of the amide I band based on the β-sheet structure (1627 cm^{-1}) for the RA spectrum was quite smaller than that for the TM spectrum. The TM method emphasizes vibrational modes parallel to the film plane, the RA method those perpendicular to the surface. This enables us to calculate the mean orientational angle θ (to the vertical axis of the surface) of a vibrational transition moment using the Equation (2):

$$A_T/A_R = \sin^2\theta/(2m_z \times \cos^2\theta) \quad (2)$$

where m_z is the enhancement factor of reflection spectra with respect to transmission spectra, and A_T and A_R are the transmission and reflection absorbance of amide I (1627 cm^{-1}) normalized with the absorbance for the C=O stretching band of ester group (1740 cm^{-1}), respectively.[42] As a result, the average angle (θ) of β-sheet amide I band (C=O stretching) was estimated to be about 85°; in other words, the amide bonding of peptide chain was formed parallel to the substrate surface. AFM study revealed that most of **1**-fibril was adsorbed parallel to the surface of solid substrate (Figure 4e). Considering this finding, the obtained value of θ indicates the presence of a regular structure, in which the constituent β-strands run perpendicular to the long axis of a fiber and their hydrogen bondings run parallel to this axis as they do in an amyloid core structure.

An amyloid-like ordered structure of **1**-fibril was also supported strongly by Congo red (CR) binding study. CR is a sulfonated azo dye that binds preferentially, but not exclusively, to protein and peptide species adopting a cross-β amyloid structure.[43] CR-stained amyloids show a green birefringence under polarized light; this suggests that the bound CR molecules are ordered with respect to each other. This effect is caused by the regular structure of the amyloids.[44] Figure 6 shows an optical microscope image obtained under cross-polarized light and containing the peptide **1** fibril stained with CR.

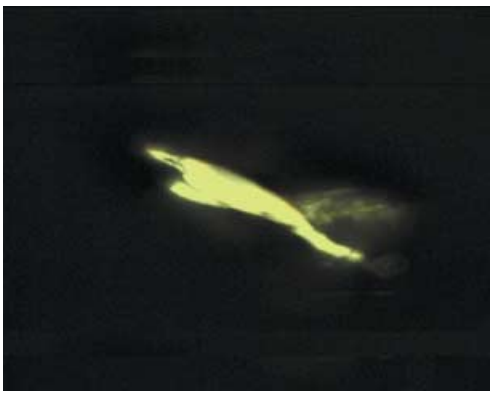

Figure 6. Optical microscope image obtained under cross-polarized light and containing the peptide **1**-fibril stained with Congo red. The fibrillar **1**-assembly was obtained after 48 h incubation in water/TFE (8:2 *v*/*v*) at pH 4.0.

  0947-6539/03/0905-1151 $ 20.00+.50/0

The stained peptide assemblies exhibited a yellow-green birefringence under cross-polarized light. Although the birefringence differs somewhat from the green birefringence of amyloid,[43, 44] it is a clear indication of their anisotropy and therefore indicates the presence of a regular quaternary structure.

Conformational regulation of peptide-conjugated copolymer by interacting with poly(ethylene glycol) derivatives: Both the conformation and the morphology of peptide **1** in solution were affected strongly by environmental conditions such as solution composition and pH. It is therefore expected that the distribution of high-order structures of the amyloidogenic synthetic peptide can be controlled by using interaction with amphiphilic compounds that affect the aggregation behavior of peptide chains. We focused on the poly(ethylene glycol) (PEG) derivatives as a "conformation regulator". PEG is an important biocompatible amphiphilic polymer because of its non-toxicity and non-antigenic activity. In addition, PEG derivatives are known to stabilize or preserve the three-dimensional structure of proteins and in some cases even to induce random chain polypeptides to form helical structures through the hydrophobic interaction.[45, 46] In this study, two types of PEG derivatives, possessing a carboxyl group (PEG-COOH) or an amino group (PEG-NH_2) at their ω-termini, were used to regulate the strength of an interaction with **1**, which was possible as a result of the electrostatic interaction. First, we examined the inhibition effects of these PEG derivatives on the α-to-β structural transition of peptide **1**. Figure 7 shows the helicity change of peptide **1** with time in the absence and the presence of PEG derivatives in water/TFE (8:2 *v*/*v*) at various pHs (helicity was estimated from CD measurement). The addition of carboxyl-terminated PEG derivative revealed a significant inhibition of the α-to-β structural transition of peptide **1** based on the pH of the solution (Figure 7b–d), compared with the case in which no such PEG derivatives were added (Figure 7a). In particular, in the case of pH 6.8 (Figure 7d), an α-helix structure was maintained at about 60% content even after incubation for 24 h. In this case, peptide **1** did not form amyloid-like fibril structures (from AFM measurement, data not shown). Moreover, it should be noted that the enhancement in helicity of **1** was observed in the presence of PEG derivative at the initial stage, indicating the direct interaction between hydrophobic PMLG segments and PEG segments. Based on the results of these pH-dependent inhibitions, it can be considered that the interaction between carboxyl and amino groups of **1** occur via the electrostatic interaction. In fact, in the case of PEG-NH_2, which has no anionic groups, the pronounced inhibition of the α-to-β structural transition of peptide **1** was not observed under the same condition used to observe PEG-COOH (Figure 7e–g). Thus, it seems possible to prevent tight packing among hydrophobic peptides and subsequent fibril formation, based on the efficient interaction between **1** and PEG, which could be enhanced by utilizing an intermolecular attractive force such as an ion complex.

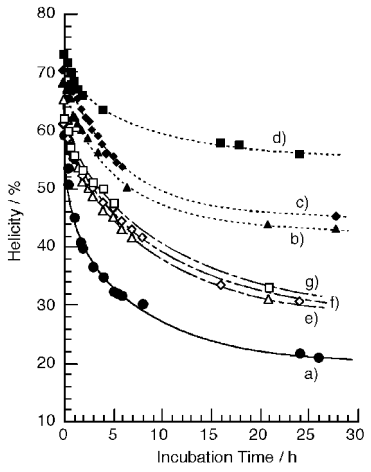

Figure 7. Time dependence of helicity of peptide **1** in water/TFE (8:2 *v*/*v*) under the following conditions: a) at pH 4.0 without PEG derivatives, b) at pH 4.0 with PEG-COOH, c) at pH 5.4 with PEG-COOH, d) at pH 6.8 with PEG-COOH, e) at pH 4.0 with PEG-NH_2, f) at pH 5.4 with PEG-NH_2, and g) at pH 6.8 with PEG-NH_2. [MLG] = 1.1×10^{-4} unit M. [PEG derivatives]:[amine unit of **1**] = 1:1.

We also investigated the additional effects of PEG derivative on the conformation of peptide **1**-assembly in β-sheet form. Figure 8 shows the CD spectral change of **1**-fibril in β-sheet form with the addition of PEG-COOH in water/TFE (8:2 *v*/*v*) at pH 6.8. As suggested above, PEG-COOH is able to interact efficiently with peptide **1** under this condition. Interestingly, the partial conversion, from β-sheet to α-helix, took place with incubating (0–48 h), as evidenced by an increased in the negative ellipticity at 208 nm and an increase in the positive ellipticity at 193 nm. Prolonged incubation did not further promote the transition. Thus, this interaction between **1**-fibril and PEG derivative does not cause the perfect transition into an α-helix structure as was observed for **1** before β-sheet formation. These results, however, suggest the possibility of using PEG derivatives not only as an inhibitor of the α-to-β structural transition of peptide **1** but also as a stabilizer for the α-helix structure, because they have an ability to induce a partial conversion from β-sheet to α-helix.

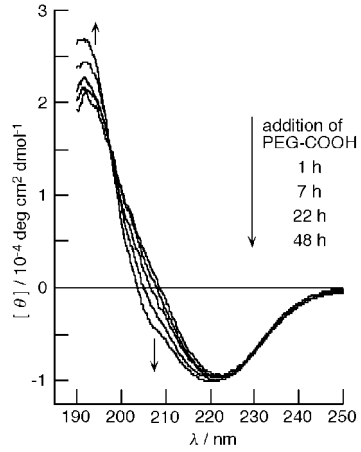

Figure 8. Molecular interaction-induced secondary structural transition in peptide **1**. The peptide **1** was incubated for 48 h in water/TFE (8:2 *v*/*v*) at pH 6.8, then PEG-COOH was added to this solution. The far-UV CD spectral change was measured at the indicated time periods (0–48 h) after addition of PEG-COOH. [MLG] = $1.1 \times 10-4$ unit M. [PEG-COOH]:[amine unit of 1] = 1:1.

0947-6539/03/0905-1152 $ 20.00+.50/0 *Chem. Eur. J.* **2003**, *9*, No. 5

Discussion

Effects of environmental conditions on the amyloid-like fibril formation: The present results indicate that the properties of the aggregates formed by artificial protein, hydrophobic PMLG-conjugated cationic polyamine **1**, are highly dependent on environmental conditions such as the solution composition, pH, and salt concentration in which aggregation takes place. The ability to control the distribution of high-order structures formed by manipulating such environmental conditions provides insights into the assembly mechanism. Figure 9 illustrates schematically the morphology and the conformation of peptide **1** in solutions. In

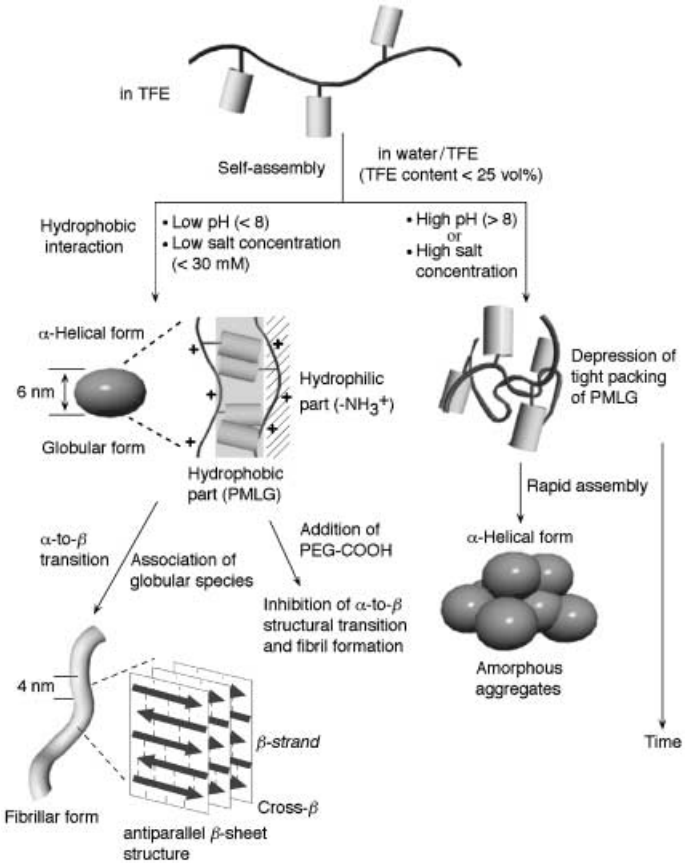

Figure 9. Schematic illustration of morphology and conformation of peptide **1** in water/TFE solution.

aqueous solution (< TFE 25%), the peptides **1** were self-assembled and formed the aggregates, whereas **1** existed as a monomer in TFE solution (Table 1, Figure 3B). These findings indicated that the aggregation of **1** took place via the strong hydrophobic interaction between PMLG chains, which acted as a main driving force for assembly. The distribution of high-order structures and the aggregation behaviors of these assemblies were restricted by pH and ionic strength at this stage. Far-UV CD and FTIR spectra of peptide **1** demonstrated that an α-helix conformation is self-converted into antiparallel β-sheet one under the condition of lower pH (< 8: protonation of amino groups) and at lower salt concentration (< 30 mM). Generally, PMLG has been known to form a stable α-helix structure, and the β-sheet formation would require a particular, harsh condition (e.g., high temperature, mechanical stress). Thus, such a conformation for PMLG may not be primarily so stable. In this case, however, the amphiphilic property of peptide **1** causes tight packing of hydrophobic PMLG chains under the acidic condition, then the intramolecular hydrogen bonding is likely to be rearranged into the intermolecular one, which induces the conformation change of PMLG chain from α-helix to β-sheet. In parallel with these changes in conformation, FRET studies indicate progress of aggregate formation of peptides **1** without a lag time (Figure 3). A nucleation-dependent polymerization model has been proposed to explain the mechanisms of amyloid formation by a variety of disease-related proteins,[47–49] and it has been well established as the fundamental mechanism of crystal growth.[50] In this model, nucleus formation require a step involving association with protein monomers that is thermodynamically unfavorable, and as a result a marked lag phase has been observed before aggregation and/or conformational transition of proteins and peptides. In our case, however, no such lag phase before fibril formation of **1** was observed under any experimental conditions. These differences in aggregation kinetics between peptide **1** and authentic amyloids can be explained as follows. The peptide chains of **1** are composed of highly hydrophobic γ-methyl-L-glutamate, and the peptide chains are already forced to assemble on a flexible polymer template. Therefore, it can be assumed that the nucleus formation steps of **1**, which are based on hydrophobic interaction of PMLG segments, were accelerated remarkably in aqueous media (namely, nucleus formation was supposed to occur just after preparation of sample solution), and as a result the lag phase could not be apparently detected. In fact, it has been reported that the addition of a previous formed aggregate (nucleus) to a solution of monomeric amyloidogenic peptide reduces or entirely eliminates the lag phase in aggregate growth in the case of Aβ peptide.[48]

AFM measurements provide further information on the process of fibril formation of **1**. The peptide **1** was found to form globular aggregates about 6.0 nm in height when the peptide was dissolved in aqueous solution (Figure 4a). These globular species are probably micellar structures consisting of a hydrophobic PMLG core and the shell of a protonated-allylamine unit. In addition, taking into account the fact that the conformation of **1** was finally converted into an antiparallel β-sheet structure, α-helical PMLG chains of **1** were assumed to fold in an antiparallel side-by-side orientation in this globular form. This orientation of the polypeptides can be explained in view of a helix macrodipole. The dipole moments of amino acid in an α-helical peptide align in the same direction, nearly parallel to the helix axis, then the resulting macroscopic dipole generates an electrostatic potential, directed from the N-terminus to the C-terminus.[51, 52] This electrostatic field plays an important role in the high-order structure and functions of proteins. Niwa et al. reported direct evidence for helix–helix macrodipole interaction by exploring an attractive interaction between the disulfide-modified poly(L-glutamic acid) self-assembled monolayer on gold and redox active poly(L-glutamic acid) derivatives as guest

helices.[53] Thus, the helix-macrodipole interaction (namely, the head-to-tail antiparallel orientation of the PMLG chain, which is energetically more favorable) probably also contributes to the stability of the high-order structure of **1**-aggregate at the initial stage (globular form) as well as to the hydrophobic interaction between α-helical PMLGs in aqueous solution. Amyloid-like fibrils (ca. 4 nm) that possess a well-defined three-dimensional regular structure (cross β) were constructed through the process of molecular association between the globular species, which is observed in authentic amyloids (Figure 4c).

On the other hand, at higher pH (> 8) region or higher salt concentration (> 30 mM), the peptide **1** was assembled rapidly with α-helical conformation and formed poorly organized amorphous aggregates (Figure 3B b), Figure 4f). At high pH or high salt concentration, the positive charges present on the peptide **1** will be screened or disappeared (pK_a of amino groups of PAA segment: ca. 8.0). This increased tendency for intermolecular interactions between peptides **1**, which caused rapid aggregation of **1**, is due to a drastic decrease in electrostatic repulsion and an increase in hydrophobicity. Moreover, rapid aggregation of **1** seems to restrict mobility of the polypeptide chains, resulting in prevention of appropriate folding of polypeptide chains (tight packing of peptides) necessary for conformational transition. On the other hand, formation of highly organized fibrils requires the development of regular intermolecular interactions involving extended regions of polypeptide chain, which interactions are observed for positively charged peptide **1** at low pH and low salt concentration. This charge will probably provide sufficient intermolecular repulsion to permit controlled growth of fibrils as well as sufficient mobility of peptide chains for appropriate folding. A similar situation was observed for non-pathogenic protein, the SH3 domain of PI3-SH3, and the authors also noted the importance of regular intermolecular interactions for fibril formation which could be restricted by charge of the side chains of amino acids.[54] These concepts will also be supported by the fact that many proteins form amyloid fibrils when they possess a substantial net charge on the protein.[14, 55, 56] These studies undoubtedly will make an important contribution to our understanding of the mechanism of protein aggregation and amyloid fibril formation.

Intermolecular interaction controls the high-order structure of aggregates: The presence of particular PEG derivatives demonstrated obvious inhibition of the α-to-β conversion for non-assembled peptide **1**, and for assembled peptide **1** even partially induced helical structure in β-sheet peptide. In order to understand the therapeutics for amyloid disease, it seems important to control the high-order structure of peptides through external stimuli such as intermolecular interaction; namely, through development of a conformation regulator. In the case of peptide **1**, an aggregation between hydrophobic peptide segments is the first key step for well organized fibril formation. In this regard, we chose a conformation regulator, carboxyl-terminated PEG derivatives, based on the following criteria: i) existence of an amphiphilic part that could interact with the hydrophobic peptide domain; ii) introduction of a functional group that would permit the effective approach of the amphiphilic part into the neighborhood of the target peptide domain via attractive force. The pH dependence of the inhibition effect of the α-to-β structural transition of **1** and enhancement in helicity of **1** observed upon addition of PEG-COOH indicated the importance of both the PEG segment and the carboxyl group, as expected (Figure 7). That is, the carboxylate anion promotes effective interaction through the ion complexation with amino cation of **1**, and the PEG segment prevents tight aggregation among polypeptide chains by interacting with the hydrophobic PMLG chain directly and contributes to the stabilization of the α-helix structure. Such direct PEG–peptide interaction also partially induces the β-to-α structural transition of **1**-assembly (Figure 8). It has been considered that proteins and peptides that are intrinsically not rich in the β-sheet characteristic can undergo a transition from a β-sheet to an α-helix structure. Only a few previous reports have described a β-to-α structural transition, achieved by manipulating the solution composition[57] or temperature.[58] In contrast, it is postulated that secondary structural transitions occur in which a cleaved segment of a protein that is normally found in an α-helical form is converted to a stable β-sheet in a disease state such as scrapie or Alzheimer's disease.[5–8, 59] Many researchers believe that these protein conformation changes are central to the disease process. Therefore, these phenomena of β-to-α transition observed in the peptide **1** model system might provide new insights for controlling peptide conformation and contribute to the therapeutics for amyloid disease, although our findings did not yield a conclusive mechanism by which to explain such a β-to-α transition. Moreover, approaches using a conformation regulator such as the PEG derivatives would be expected to be applicable to disease-related peptides such as the Aβ peptide, since it has also been assumed that hydrophobic defects, which derive from the hydrophobic amino acid sequence, induce molecular aggregation for many amyloidogenic peptides including Aβ peptide.[5–8] Further work concerning the conformation regulator are now in progress.

Conclusion

In the present study we successfully synthesized a novel artificial protein model, polyglutamate-grafted polyallylamine, and described its structural and conformational properties in solutions. The secondary and quaternary structures of the peptide **1** can be easily controlled by manipulating the pH, solution composition, and salt concentration. Only under the condition of low pH (< 8) or that of low salt concentration (< 30 mM) did the electrostatic repulsive force based on the protonated amino groups permit the controlled growth of **1**-aggregates and the tight packing of hydrophobic PMLG chains, resulting in induction of highly ordered fibril formation with α-to-β structural transition. These findings strongly suggest that the formation of fibril structure is not restricted to specific protein sequences but is, rather, a common property of polypeptides, although the appropriate packing arrangement of peptide chains is required. In addition, poly(ethylene glycol) derivative was found to act as a "conformation regulator" through direct interaction with the hydrophobic

0947-6539/03/0905-1154 $ 20.00+.50/0 *Chem. Eur. J.* **2003**, *9*, No. 5

peptide segment of **1**, preventing tight packing of peptides and stabilizing their α-helical structure. We believe the ability to control the distribution of high-order structures of the model peptide formed by manipulating environmental conditions or intermolecular interaction provides important insights not only for understanding the assembly mechanism of peptides and proteins including amyloid formation, but also for developing novel peptide-based material with well-defined nanostructures for use in material science and engineering.

Experimental Section

Materials: Amyloidogenic peptide, poly(γ-methyl-L-glutamate) grafted polyallylamine (**1**), was prepared as follows (see Scheme 1). First, polyallylamine (PAA, $M_w = 10\,000$, Nittobo) (1.00 g) was dissolved in water (10 mL, pH 9.5), then a dioxane solution (10 mL) of di-*tert*-butyl dicarbonate (0.96 g) was added slowly. After stirring for 8 h at room temperature, 1M NaOH solution (50 mL) was added into the reaction mixture, then the precipitate was washed with water and lyophilized. As a result, the PAA copolymer in which the amino groups (40%) were protected with Boc groups (Boc-$PAA_{0.4}$-*co*-$PAA_{0.6}$) was obtained (1.42 g). The ratio of the free amino groups to the Boc-protected amino groups was estimated by means of ^{1}H NMR spectroscopy on the basis of the area ratio of the signal of -CH_2-NH_2 to that of -CH_2-NHCO- in the PAA side chain. Subsequently, graft-polymerization of γ-methyl-L-glutamate-*N*-carboxy anhydride (MLG-NCA) was carried out using free amino groups of the Boc-PAA-*co*-PAA. The MLG-NCA was synthesized by reacting triphosgene with γ-methyl-L-glutamate in THF.[25] MLG-NCA (1.32 g) and Boc-PAA-*co*-PAA (0.05 g) was added in chloroform (150 mL), and the solution was stirred for 40 h at room temperature. Then the reaction mixture was poured into a large excess of diethyl ether, and the precipitate (Boc-PAAgPMLG) was repeatedly washed with diethyl ether and 1,2-dichloroethane (0.80 g). The chemical structure of Boc-PAAgPMLG was confirmed by IR, ^{1}H NMR spectroscopy and by elemental analyses. The graft-polymerization was found to proceed for all amino groups of Boc-PAA-*co*-PAA on the basis of the disappearance of the CH_2 signal adjacent to the amino group in the ^{1}H NMR spectrum. In addition, the number-average degree of polymerization (n) of the PMLG graft chain was estimated to be 14 on the basis of the area ratio of the signal of CH_3 in the Boc group to that of CH_3 in the PMLG segment. Finally, the desired PMLG-grafted PAA (**1**) was obtained by removal of the Boc groups in trifluoroacetic acid solution to yield 0.62 g. The chemical structure of **1** was confirmed by ^{1}H NMR analysis.

The peptide **1** containing nitrobenzofurazan at the amino groups of the PAA unit (**1**-NBD) was obtained as follows. The peptide **1** (50 mg) was dissolved in TFE/water (5 mL; 1:1 *v*/*v*, pH 11.0), and 4-fluoro-7-nitrobenzofurazan (NBD-F, 0.55 mg) in ethanol (30 μL) was added into the reaction mixture. The molar ratio of NBD-F to amino groups of **1** was 0.1. After incubation for 1 min at 60 °C, this solution was rapidly quenched to 0 °C and dialyzed against water/ethanol (1 L; 6:4 *v*/*v*) using a Spectra/Pore molecular porous membrane tube (Spectrum Medical Industries, Inc., MWCO 3500). After the dialysis, the solution was lyophilized to obtain **1**-NBD (35 mg). The peptide **1** containing Rhodamine B at the amino groups of the PAA unit (**1**-RhB) was obtained by treating peptide **1** (50 mg) with RhB isothiocyanate (1.60 mg) in TFE/water (1:1 *v*/*v*, pH 11.5), and purified by dialyzing against water/ethanol (1 L; 6:4 *v*/*v*) in a manner similar to that described above to yield 37 mg. The degrees of introduction of NBD and RhB to the amino groups of peptide **1** were estimated to be 5.1 and 4.9%, respectively, from UV-absorbance at 463 nm (NBD) and 548 nm (RhB) in 2,2,2-trifluoroethanol (TFE).

The α-methoxy-ω-carboxyl-poly(ethylene glycol) (PEG-COOH, av M_w: 5000) and the α-methoxy-ω-amino-poly(ethylene glycol) (PEG-NH_2, av M_w: 5000) were purchased from Sigma and Funakoshi, respectively, and used without further purification.

Far-UV/CD and FTIR spectroscopy measurements: Far-UV CD spectra were recorded on a J-720 WI spectropolarimeter (JASCO) under a nitrogen atmosphere. Experiments were performed in a quartz cell with a 5 mm path length over the range of 190–250 nm at ambient temperature. Sample solutions were prepared by diluting the TFE stock solution of peptide **1** with purified water. Final peptide concentration was 1.1×10^{-4} glutamate unit M in aqueous media. The pH of the sample solution was adjusted with 0.1M HCl or 0.1M NaOH. The helicity was calculated by using a curve-fitting method (Greenfield et al.).[26] Transmission-FTIR spectra were measured with the Perkin–Elmer Spectrum 2000, using a mercury/cadmium/tellurium (MCT) detector (resolution: 2 cm^{-1}; number of scans: 1024). Reflection absorption spectra were obtained on an Au-deposited glass plate using a MCT detector (resolution: 2 cm^{-1}; number of scans: 1024). The *p*-polarized light was introduced onto the sample at 80° to the surface normal. The sample and the detector chamber were purged with dried nitrogen before and during measurement.

AFM measurement: The AFM images were collected at ambient temperature on a Nanoscope IIIa (Digital Instrument, Inc.) operated in a tapping mode using silicon cantilevers (125 μm, tip radius 5–10 nm). An aliquot of **1** in water/TFE solution was placed on freshly cleaved mica. After adsorption for 3 min, the excess solution was removed by absorption onto filter paper. A 10 μm × 10 μm scanner was used for imaging. The scanning speed was at a line frequency of 1 Hz, and the original images were sampled at a resolution of 512 × 512 points.

Fluorescence spectroscopy measurement: Fluorescence spectra of a solution of **1**-NBD and **1**-RhB (1:1 *v*/*v*) were measured on a RF-5300 PC fluorescence spectrophotometer (Shimadzu, Japan) at a wavelength of 465 nm for NBD excitation. Experiments were performed at room temperature in a quartz cell with a 10 mm path length. In order to investigate the fluorescent resonance energy transfer from NBD to RhB, fluorescence spectra were obtained by subtracting the spectra of **1**-RhB from that of **1**-NBD/**1**-RhB solution, since only the RhB gave a small amount of fluorescence when the solution was excited at 465 nm.

Congo red binding study: A Congo red (Wako Pure Chemical Industries) stock solution (150 μM) was prepared by dissolving the dye in water/TFE (8:2 *v*/*v*) containing NaCl. The fibrillar **1**-assembly was prepared by incubating the sample solution for 48 h at room temperature as described above. Binding studies were carried out by diluting the **1** solution (after a 48 h incubation) with the Congo red solution. The final concentration of Congo red was 3 μM in water/TFE (8:2 *v*/*v*) at pH 4.0 and containing 100 mM NaCl. The resulting solution was incubated at room temperature for 3 h, and 50 μL of the solution was placed on a microscope slide and dried. The slide was examined under a microscope (Olympus Optical, BX50-34-FLAD-1) with cross-polarized light (magnification 1000 ×).

[1] P. Y. Chou, G. D. Fasman, *Biochemistry* **1974**, *13*, 222–245.
[2] R. W. Williams, A. Chang, D. Juretic, S. Loughran, *Biochim. Biophys. Acta* **1987**, *916*, 200–204.
[3] D. Minor, P. S. Kim, *Nature* **1994**, *371*, 264–267.
[4] J. D. Sipe, *Crit. Rev. Clin. Lab. Sci.* **1994**, *31*, 325–354.
[5] J. W. Kelly, *Curr. Opin. Struct. Biol.* **1998**, *8*, 101–106.
[6] P. T. Lansbury, *Proc. Natl. Acad. Sci. USA* **1999**, *96*, 3342–3344.
[7] C. M. Dobson, *Trends Biochem. Sci.* **1999**, *24*, 329–332.
[8] L. C. Serpell, *Biochim. Biophys. Acta* **2000**, *1502*, 16–30.
[9] D. R. Howlett, K. H. Jennings, D. C. Lee, M. S. G. Clark, F. Brown, R. Wetzel, S. J. Wood, P. Camilleri, G. W. Roberts, *Neurodegeneration* **1995**, *4*, 23–32.
[10] A. Lorenzo, B. A. Yankner, *Proc. Natl. Acad. Sci. USA* **1994**, *91*, 12243–12247.
[11] C. J. Pike, D. Burdick, A. J. Walencewicz, C. G. Glabe, C. W. Cotman, *J. Neurosci.* **1993**, *13*, 1676–1687.
[12] J. C. Rochet, P. T. Lansbury, *Curr. Opin. Struct. Biol.* **2000**, *10*, 60–68.
[13] M. Sunda, C. C. F. Blake, *Adv. Protein Chem.* **1997**, *50*, 123–159.
[14] J. I. Guijarro, M. Sunda, J. A. Jones, I. D. Campbell, C. M. Dobson, *Proc. Natl. Acad. Sci. USA* **1998**, *95*, 4224–4228.
[15] F. Chiti, P.Webster, N. Taddei, A. Clark, M. Stefani, G. Ramponi, C. M. Dobson, *Proc. Natl. Acad. Sci. USA* **1999**, *96*, 3590–3594.
[16] M. Fandrich, M. A. Fletcher, C. M. Dobson, *Nature* **2001**, *410*, 165–166.
[17] H. A. Lashuel, S. R. LaBrenz, L. Woo, L. C. Serpell, J. W. Kelly, *J. Am. Chem. Soc.* **2000**, *122*, 5262–5277.
[18] Y. Takahashi, A. Ueno, H. Mihara, *Chem. Eur. J.* **1998**, *4*, 2475–2484.

  0947-6539/03/0905-1155 $ 20.00+.50/0

[19] Y. Fezoui, D. M. Hartley, D. M. Walsh, D. J. Selkoe, J. J. Osterhout, D. B. Teplow, *Nat. Struct. Biol.* **2000**, *7*, 1095 – 1099.
[20] S. Chen, V. Berthelier, J. B. Hamilton, B. O'Nuallain, R. Wetzel, *Biochemistry* **2002**, *41*, 7391 – 7399.
[21] T. Koga, K. Taguchi, T. Kinoshita, M. Higuchi, *Chem. Commun.* **2002**, 242 – 243.
[22] C. E. MacPhee, C. M. Dobson, *J. Am. Chem. Soc.* **2000**, *122*, 12707 – 12713.
[23] O. Rathore, D. Y. Sogah, *J. Am. Chem. Soc.* **2001**, *123*, 5231 – 5239.
[24] Y. Takahashi, A. Ueno, H. Mihara, *ChemBioChem* **2002**, *3*, 637 – 642.
[25] W. H. Daly, D. Poche, *Tetrahedron Lett.* **1988**, *29*, 5859 – 5864.
[26] N. Greenfield, G. D. Fasman, *Biochemistry* **1969**, *8*, 4108 – 4116.
[27] M. Mutter, S. Vuilleumier, *Angew. Chem.* **1989**, *101*, 551 – 692; *Angew. Chem. Int. Ed. Engl.* **1989**, *28*, 535 – 554.
[28] T. Sasaki, E. T. Kaiser, *J. Am. Chem. Soc.* **1989**, *111*, 380 – 381.
[29] R. M. Ghadiri, C. Soares, C. Choi, *J. Am. Chem. Soc.* **1992**, *114*, 825 – 831.
[30] P. Wallimann, R. J. Kennedy, D. S. Kemp, *Angew. Chem.* **1999**, *111*, 1377 – 1379; *Angew. Chem. Int. Ed.* **1999**, *38*, 1290 – 1292.
[31] N. Higashi, T. Koga, N. Niwa, M. Niwa, *Chem. Commun.* **2000**, 361 – 362.
[32] S. Sakamoto, A. Ueno, H. Mihara, *Chem. Commun.* **2000**, 1741 – 1742.
[33] N. Higashi, T. Koga, M. Niwa, *ChemBioChem* **2002**, *3*, 448 – 454.
[34] M. Higuchi, J. P. Wright, K. Taguchi, T. Kinoshita, *Langmuir* **2000**, *16*, 7061 – 7067.
[35] D. J. Gordon, *Biochemistry* **1972**, *11*, 413 – 420.
[36] G. Conio, E. Patrone, S. J. Brighetti, *J. Biol. Chem*. **1970**, *245*, 3335 – 3340.
[37] R. W. Storrs, D. Truckses, D. E. Wemmer, *Biochemistry* **1992**, *32*, 1695 – 1702.
[38] A. Cammers-Goodwin, T. J. Allen, S. L. Oslick, K. M. McClure, J. H. Lee, D. S. Kemp, *J. Am. Chem. Soc.* **1996**, *118*, 3082 – 3090.
[39] K. A. Ramirez-Aguilar, K. L. Rowlen, *Langmuir* **1998**, *14*, 2562 – 2566.
[40] J. D. Harper, S. S. Wong, C. M. Lieber, P. T. Lansbury, *Biochemistry* **1999**, *38*, 8972 – 8980.
[41] T. Miyazawa, E. R. Blout, *J. Am. Chem. Soc.* **1961**, *83*, 712 – 719.
[42] J. Umemura, T. Kamata, T. Kawai, T. Takenaka, *J. Phys. Chem.* **1990**, *94*, 62 – 67.
[43] H. Puchtler, F. Sweat, M. Levine, *J. Histochem. Cytochem.* **1962**, *10*, 355 – 364.
[44] J. H. Cooper, *Lab. Invest.* **1974**, *31*, 232 – 238.
[45] A. Harada, S. Cammas, K. Kataoka, *Macromolecules* **1996**, *29*, 6183 – 6188.
[46] K. P. Pemawansa, A. Thakur, E. K. Karikari, T. M. Khan, *Macromolecules* **1999**, *32*, 1910 – 1917.
[47] J. T. Jarrett, P. T. Lansbury, *Biochemistry* **1992**, *31*, 12345 – 12354.
[48] J. D. Harper, P. T. Lansbury, *Annu. Rev. Biochem.* **1997**, *66*, 385 – 407.
[49] A. Lomakin, D. S. Chung, G. B. Benedek, D. A. Kirschner, D. B. Teplow, *Proc. Natl. Acad. Sci. USA* **1996**, *93*, 1125 – 1129.
[50] D. M. Blow, N. E. Chayen, L. F. Lloyd, E. Saridakis, *Protein Sci.* **1994**, *3*, 1638 – 1643.
[51] A. Wada, *Adv. Biophys.* **1976**, *9*, 1 – 63.
[52] W. G. J. Hol, P. T. van Duijnen, H. T. C. Berendsen, *Nature* **1978**, *273*, 443 – 446.
[53] M. Niwa, M. Morikawa, N. Higashi, *Langmuir* **1999**, *15*, 5088 – 5092.
[54] J. Zurdo, J. I. Guijarro, J. L. Jimenez, H. R. Saibil, C. M. Dobson, *J. Mol. Biol.* **2001**, *311*, 325 – 340.
[55] V. Villegas, J. Zurdo, V. V. Filimonov, F. X. Aviles, C. M. Dobson, L. Serrano, *Protein Sci.* **2000**, *9*, 1700 – 1708.
[56] S. P. Martsev, A. P. Dubnovitsky, A. P. Vlasov, M. Hoshino, K. Hasegawa, H. Naiki, Y. Goto, *Biochemistry* **2002**, *41*, 3389 – 3395.
[57] S. Zhang, A. Rich, *Proc. Natl. Acad. Sci. USA* **1997**, *94*, 23 – 28.
[58] E. Kauffmann, N. C. Darnton, R. H. Austin, C. Batt, K. Gerwert, *Proc. Natl. Acad. Sci USA* **2001**, *98*, 6646 – 6649.
[59] S. B. Prusiner, *Science* **1991**, *252*, 1515 – 1522.

Received: September 20, 2002 [F4439]

  0947-6539/03/0905-1156 $ 20.00+.50/0